AD-A194 017 COMPUTATION OF LOW SPEED VISCOUS FLOWS WITH HEAT ADDITION(U) PENNSYLVANIA STATE UNIV UNIVERSITY PARK DEPT OF MECHANICAL ENGINEERING A HOSANGADI ET AL. 1986 1/1

UNCLASSIFIED AFOSR-TR-88-0468 AFOSR-84-0048 F/G 20/4 NL

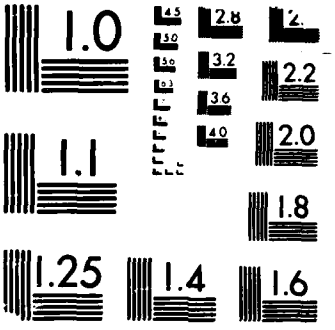

AD-A194 017

REPORT DOCUMENTATION PAGE

1a. REPORT SECURITY CLASSIFICATION: Unclassified	1b. RESTRICTIVE MARKINGS: DTIC FILE COPY
2a. SECURITY CLASSIFICATION AUTHORITY	3. DISTRIBUTION/AVAILABILITY OF REPORT: Approved for Public Release Distribution is Unlimited
2b. DECLASSIFICATION/DOWNGRADING SCHEDULE: NA	
4. PERFORMING ORGANIZATION REPORT NUMBER(S): None	5. MONITORING ORGANIZATION REPORT NUMBER(S): AFOSR-TR- 88-0468
6a. NAME OF PERFORMING ORGANIZATION: Pennsylvania State University	6b. OFFICE SYMBOL (If applicable):
6c. ADDRESS (City, State and ZIP Code): Mechanical Engineering Dept. University Park, PA 16802	7a. NAME OF MONITORING ORGANIZATION: AFOSR
	7b. ADDRESS (City, State and ZIP Code): Same as 8c.
8a. NAME OF FUNDING/SPONSORING ORGANIZATION: Air Force Office of Scientific Research	8b. OFFICE SYMBOL (If applicable): NA
	9. PROCUREMENT INSTRUMENT IDENTIFICATION NUMBER: AFOSR-84-0048
8c. ADDRESS (City, State and ZIP Code): Bldg 410 Bolling AFB, Washington, D.C. 20332	10. SOURCE OF FUNDING NOS.

PROGRAM ELEMENT NO.	PROJECT NO.	TASK NO.	WORK UNIT NO.
61102F	2308	A1	

11. TITLE (Include Security Classification): Computation of Low Speed Viscous Flows with Heat Addition

12. PERSONAL AUTHOR(S): Ashvin Hosangadi and Charles L. Merkle

13a. TYPE OF REPORT	13b. TIME COVERED	14. DATE OF REPORT (Yr., Mo., Day)	15. PAGE COUNT
Article	FROM _____ TO _____		5

16. SUPPLEMENTARY NOTATION

DTIC ELECTE MAY 04 1988 S D

17. COSATI CODES			18. SUBJECT TERMS (Continue on reverse if necessary and identify by block number)
FIELD	GROUP	SUB. GR.	

19. ABSTRACT (Continue on reverse if necessary and identify by block number)

The use of implicit time-dependent schemes for the numerical solution of low speed, low Reynolds number flows with heat addition is investigated. Stability analyses show that the errors introduced by approximate factorization give rise to instability at Reynolds numbers around 100. Specifically, it is the cross-derivative errors between the viscous and inviscid terms that cause problems. When exact inversion techniques are used, the system becomes strongly stable and numerical experiments show rapid convergence. Comparisons of outflow boundary conditions show that viscous and inviscid formulations give identical results over a wide range of Reynolds numbers when buoyancy is omitted, but with buoyancy present the inviscid boundary conditions are unstable. Flowfield results for a range of low Reynolds conditions with and without buoyancy are given to show the manner in which the flowfield changes as these physical parameters are varied.

20. DISTRIBUTION/AVAILABILITY OF ABSTRACT	21. ABSTRACT SECURITY CLASSIFICATION
UNCLASSIFIED/UNLIMITED [X] SAME AS RPT. [ ] DTIC USERS [ ]	Unclassified

22a. NAME OF RESPONSIBLE INDIVIDUAL	22b. TELEPHONE NUMBER (Include Area Code)	22c. OFFICE SYMBOL
Dr. Mithat Birkan	(202) 767-4938	AFOSR/NA

DD FORM 1473, 83 APR EDITION OF 1 JAN 73 IS OBSOLETE.

SECURITY CLASSIFICATION OF THIS PAGE UNCLASSIFIED

COMPUTATION OF LOW SPEED VISCOUS FLOWS WITH HEAT ADDITION

Ashvin Hosangadi* and Charles L. Merkle**
The Pennsylvania State University
Department of Mechanical Engineering
University Park, PA 16802

ABSTRACT

The use of implicit time dependent schemes for the numerical solution of low speed, low Reynolds number flows with heat addition is investigated. Stability analyses show that the errors introduced by approximate factorization give rise to instability at Reynolds numbers around 100. Specifically, it is the cross-derivative errors between the viscous and inviscid terms that cause problems. When exact inversion techniques are used, the system becomes strongly stable and numerical experiments show rapid convergence. Comparisons of outflow boundary conditions show that viscous and inviscid formulations give identical results over a wide range of Reynolds numbers when buoyancy is omitted, but with buoyancy present the inviscid boundary conditions are unstable. Flowfield results for a range of low Reynolds conditions with and without buoyancy are given to show the manner in which the flowfield changes as these physical parameters are varied.

INTRODUCTION

Time dependent procedures have come to be the accepted method for the numerical solution of compressible flows. The strengths of these methods arise because they are easily expressed in generalized coordinates, they allow a single procedure to be used for either viscous or inviscid flows, and they allow the use of central differences for the convective terms even when the inviscid equations are considered. Their capabilities in inviscid flows make them particularly suitable for the important class of high Reynolds number viscous flows. Recent publications[1-4] have reported effective methods for extending these compressible flow techniques to low Mach number conditions where eigenvalue stiffness had heretofore precluded convergence. The present paper looks at the additional extension to low Reynolds number flows. The physical problem used to demonstrate the low Reynolds number conditions is that of strong heat addition in a constant area duct. The source of this problem arises because of our interest in the absorption of a laser beam by a flowing gas[5].

The impaired convergence of time dependent schemes at low Mach number is known to arise because of the stiffness of the eigenvalues and the singular behavior of the pressure gradient. Preconditioning of the time derivatives[1-3] has been shown to make the convergence rate independent of Mach number, but a rescaling of the pressure is necessary[4] to ensure convergence to tight tolerances at Mach numbers below about 10^{-4}. This rescaling is best accomplished by a perturbation expansion of the equations of motion[4,6]. The presence of the source term due to buoyancy has also been shown[7] to require special treatment when Froude numbers are small.

The characteristics of time dependent schemes at low Reynolds numbers have received less attention. Although the diffusion provided by the viscous terms should smooth the solution and provide enhanced convergence, their presence can slow convergence or even lead to divergence when approximate decompositions are used in conjunction with implicit formulations. (The characteristics of approximately factored[8,9] methods are discussed herein a ; compared with results from direct inversion procedures.) In addition, the effects of inflow and outflow boundary conditions are studied to determine their effect on convergence and solution accuracy as the Reynolds number is decreased.

PROBLEM FORMULATION AND EQUATIONS OF MOTION

As a test problem, we use the flow through a vertical constant area duct with specified volumetric heat addition to simulate laser absorption in a flowing gas[5]. To parameterize the problem, the heat source, Q_H, is chosen as the algebraic function,

$$Q_H = P \text{ Min } |2f^{3/2} - 3f+1, 1| \qquad (1)$$

where,

$$f(x,y) = |(x-x_a)^2 + (y-y_a)^2|/|(x-x_b)^2 + (y-y_b)^2| \qquad (2)$$

Here P is a scaling parameter indicative of the maximum heating rate and (x_a, y_a) and (x_b, y_b) specify the coordinates about which the symmetric heat addition is centered and its rate of decrease. For the present calculations, only the peak heating rate P was varied. Cross-sectional contours of the constant heat addition curves along with the geometry of the problem is given in Fig. 1.

The equations used to describe the very low speed flows of interest here are obtained by the same Mach number expansion used in Ref. 4. Extension of this expansion to the viscous terms shows that the viscous dissipation function in the energy equation may be neglected leaving only heat conduction terms on the right-hand side and leads to no simplifications in the right-hand side of the momentum equations. The reduced equations in generalized coordinates become:

$$\partial_t Q + \partial_\xi E + \partial_\eta F = H + |\partial_\xi(R_{\xi\xi}\partial_\xi + R_{\xi\eta}\partial_\eta) + \partial_\eta(R_{\eta\xi}\partial_\xi + R_{\eta\eta}\partial_\eta)|JQ \qquad (3)$$

The notation used for the inviscid terms is the same as that of Ref. 4 while the viscous notation is similar to that of Ref. 10 with the above-mentioned simplification. The source term H contains both the heat source term and the buoyancy term.

To solve Eqn. 3 we use Euler implicit time differencing for all terms except for the cross-derivatives on the right-hand side, which are differenced explicitly. Central differencing in

*Graduate Assistant; **Professor

space is used for both the convective and diffusive terms. The implicit formulation gives rise to a large sparse, pentadiagonal matrix whose solution was attempted by the approximate factorization technique as well as by an exact, direct inversion procedure.

Approximate Factorization

The most common technique for solving implicit algorithms is the approximate factorization procedure of Douglas and Gunn[11]. In this approach, the pentadiagonal matrix is approximated by two tridiagonal matrices as,

$$(S + \Delta t\partial_\xi A - \Delta t\partial_\xi R_{\xi\xi}\partial_\xi J)S^{-1}$$

$$(S + \Delta t\partial_\eta B - \Delta t\partial_\eta R_{\eta\eta}\partial_\eta J)\Delta Q = -\Delta t R \qquad (4)$$

where R is the residual of the operator in Eqn. 3 evaluated at the old time level, and S = I-DΔt where D is the Jacobian of H.

The approximate factorization is equivalent to solving the original differential operator in Eqn. 3 with an additive error W_{AF} given by,

$$W_{AF} = \Delta t^2[\partial_\xi A\partial_\eta B + \partial_\xi R_{\xi\xi}\partial_\xi J\partial_\eta R_{\eta\eta}\partial_\eta J -$$

$$- \partial_\xi R_{\xi\xi}\partial_\xi J\partial_\eta B - \partial_\xi A\partial_\eta R_{\eta\eta}\partial_\eta J]\Delta Q \qquad (5)$$

Note this error includes terms of three kinds. There are inviscid-inviscid operator products, viscous-viscous operator products and viscous-inviscid operator products. The inviscid-inviscid terms are the familiar ones from the Euler equations. These are well known to slow convergence at high CFL's, but never cause instability or divergence. Similar comments hold for the viscous-viscous error term. In a pure diffusion equation (no convection) these terms will slow convergence but the approximately factored scheme remains unconditionally stable.

The existence of an unconditionally stable factorization for the inviscid terms alone and for the diffusion terms alone does not, however, guarantee unconditional stability for the combined viscous-inviscid system because of the viscous-inviscid error terms in Eqn. 5. Stability analyses of the complete vector equations shows that the viscous-inviscid error terms can be strongly destabilizing at moderate (order one) Reynolds numbers. At high or very low Reynolds numbers, these terms become negligible and have no effect. For our specific problem, both stability analyses and numerical experiments showed that approximate factorization was unstable at Reynolds numbers below 500 when the stiffness was removed from the inviscid terms. Making the inviscid operators stiff deferred this instability to lower Reynolds number, but the stiffness then caused unacceptably slow convergence. Thus, approximate factorization of the low Mach number equations fails at low Reynolds numbers.

Direct Solution Procedures

Analysis of the AF scheme reveals its limited usefulness at low Reynolds numbers. To understand the limitations of the approximate procedure and to provide solutions to the problem of interest, we also considered direct solutions of the operator in Eqn. 3. For these solutions, the sparse pentadiagonal matrix was partitioned as a block tridiagonal system which was then solved by the matrix version of the standard Thomas algorithm. The result requires considerable machine storage but provides an extremely robust solver as is noted below. For a two-dimensional problem, both storage and CPU time are primarily determined by the number of grid points in the smaller direction. Experimental checks on a scalar processing machine showed that when 20 to 30 grid points were used in one direction, the direct procedure gave converged solutions in about the same time as approximate factorization, albeit, at vastly different convergence rates. Thus, a grid of 50 x 25 will require nominally the same time for the direct as for the AF procedure. More advanced sparse matrix solution procedures[12] are available which would reduce storage as compared with the present tridiagonal procedure. These should also reduce the CPU time requirement.

The advantage of the direct procedure is its improved robustness and its rapid rate of convergence. Its robustness is demonstrated by the fact that converged solutions are obtained for the present problem, while appropriate procedures fail. Its rapid rate of convergence is most readily demonstrated by example. Figure 2 shows the convergence rate of the direct procedure for the present problem for a series of different CFL's. At a CFL of 5, the direct procedure converges at about the same rate as an approximate factorization scheme. (The optimum CFL for AF schemes is around 5.) As CFL is increased, the convergence rate accelerates rapidly. At a CFL of 50, convergence to machine accuracy requires only 17 iterations and at 5000, it is further reduced to 11 time steps. Tests with other grid sizes show that the rate of convergence is independent of the number of grids or even of grid stretching although the time per iteration is strongly related to the number of grids. Finally, comparison of the present rates of convergence for a two-dimensional problem with those for a one-dimensional problem show that the convergence rate is independent of the dimensionality of the problem when direct inversion is used. The normally encountered slow-down in convergence rate in multidimensions as compared to one dimension arises because of approximate factorization errors.

Boundary Conditions

The required boundary conditions for the present problem include the specification of conditions on the wall, on the axis of symmetry and on the upstream and downstream boundaries. The boundary conditions on the wall are the no-slip and adiabatic conditions. These three conditions are supplemented by an application of the normal momentum equation on the wall which is applied by using one-sided differences for the normal derivatives. At the center line, symmetry conditions are applied. Because these conditions are simple and their application is straightforward, the details are omitted.

The boundary conditions at the inlet and exit are of more interest. At high Reynolds numbers where the flow is predominantly inviscid, the use of inviscid boundary procedures appears appropriate. As the Reynolds number is decreased and viscous effects begin to dominate, the arguments for viscous boundary conditions become more compelling. The range of demarcation between these two types of boundary conditions is not immediately apparent and conclusions are based on hindsight gained from numerical experimentation.

For the inviscid limit, we use the Method of Characteristics (MOC) procedure to determine the number and type of boundary conditions. This theory

makes it clear that the variable at the boundary must be determined from a combination of formal boundary conditions augmented by a subset of the equations of motion. This rigorous understanding is lost when viscous effects are present. In cases where the inertial terms dominate, we drop normal diffusion gradients and apply the MOC procedures as though the flow were inviscid. For the present problem, these procedures corresponded to specifying the stagnation temperature, the stagnation pressure, and the flow angle at the inflow boundary and the back pressure at the outflow boundary.

For low Reynolds numbers, the procedure at the downstream boundary was changed to reflect the dominance of the viscous terms, but the lack of a rigorous procedure for determining the type of boundary conditions leads to some ambiguity as to how they are applied. The common assumption is that there will be one additional boundary condition for each addition order of derivative. Thus, the four boundary conditions of inviscid flow increase to seven boundary conditions in viscous flow. In the present calculations, the inviscid upstream boundary conditions given above were retained (with the argument that we were treating slug flow at the inlet), and the downstream specification of pressure was augmented by setting these second derivatives to zero,

$$u_{\xi\xi} = v_{\xi\xi} = T_{\xi\xi} = 0 \qquad (6)$$

so that four boundary conditions were specified at the outflow boundary.

RESULTS AND DISCUSSION

All results presented are based on the direct solution procedure. The comparison of viscous and inviscid boundary conditions is discussed first. Intuitive reasoning would suggest that the inviscid boundary conditions would hold at very high Reynolds numbers while the viscous boundary conditions would provide accurate solutions at very low Reynolds numbers. It would be hoped that both sets of boundary conditions would provide similar results for a range of intermediate Reynolds numbers. To ascertain the behavior of these boundary conditions, numerical experiments were run at Reynolds numbers of 5, 50 and 500. In the absence of buoyancy, both sets of boundary conditions gave similar convergence and similar solutions (the solutions were indistinguishable on a plot) at all three Reynolds numbers. In the presence of buoyancy, all attempts with the inviscid boundary conditions diverged at Reynolds numbers below 500 for high heat addition, but the viscous boundary conditions provided effective convergence. As is shown later, the effect of buoyancy is almost negligible at Reynolds numbers above 500 and becomes increasingly dominant at lower Reynolds numbers. (Recall, Reynolds number is being controlled by changing the velocity.)

Flowfield results for the duct flow with heat addition area given in Figs. 3-6. Results are presented for calculations with and without buoyancy, the Prandtl number being held constant at 0.7 for all cases.

Figures 3 and 4 present the temperature and velocity profiles at the exit for the non-buoyant case at Reynolds number of 5, 50 and 500. In the absence of buoyancy the heat source has a passive behavior that only causes an expansion of the gas. Low velocities abet the rapid diffusion of heat from the centerline to the wall, so that the temperature becomes essentially uniform at a Reynolds number of 5. At the higher Reynolds numbers, the reduced diffusion rates lead to steeper temperature gradients, with the heating effect being localized to the center of the flow. The velocity profiles on Fig. 4 corroborate these inferences. The rapid diffusion at the low Reynolds number case leads to a parabolic, fully developed profile. The temperature gradients at higher Reynolds numbers give rise to a fuller profile, indicating a flow which is still developing.

The corresponding profiles with buoyancy included are shown in Figs. 5 and 6. The buoyancy effect is negligible at Reynolds number 500, with the temperature and velocity profiles being almost identical to the non-buoyant case, as can be seen by comparing Figs. 3 and 5 with Figs. 2 and 4. The dramatic effect of buoyancy is, however, evident at the two lower Reynolds numbers. The center of the flow is accelerated due to heating, and the velocities at the centerline in dimensional form become comparable in magnitude to the velocity at Reynolds number 500.

The sharp decrease in the rate of diffusion at these lower Reynolds numbers is reflected in the modest temperature rise at the wall. In contrast to the non-buoyant case, the temperature profile with buoyancy at a Reynolds number of 5 is now highly non-uniform. The velocity profiles also differ quite strongly from the fully developed profiles in the non-buoyant flow. A fairly wide region near the wall has very low velocities with a tendency for flow reversal.

CONCLUSIONS

Time dependent numerical algorithms were tested for low Mach number, low Reynolds number flows with and without buoyancy. Results show that approximate factorization techniques do not converge for cases of interest. Stability analyses of these schemes indicate that the reason for the impaired performance is the hybrid Δt^2 error term that arises from the product of viscous and inviscid derivatives. Stability analyses for the unfactored algorithm indicate unconditional stability for all time step sizes, and suggest that very large Δt's will give maximum convergence when direct inversion procedures are used. The robustness of the direct inversion routine reinforces the inference that the instability encountered at low Reynolds numbers is because of the approximate factorization.

Calculations with both inviscid and viscous boundary conditions at the outflow boundary show a broad region of overlap in the ranges of application for the two procedures where buoyancy is absent. In the presence of buoyancy, the inviscid boundary conditions failed to provide solutions in Reynolds number ranges where buoyant effects were significant. The reason for this was traced to a tendency for reentry flow near the wall at the exit plane.

Flowfield solutions show that buoyancy begins to dominate at a Reynolds number of about 500. The body force due to buoyancy causes the velocity on the centerline to increase as compared with the non-buoyant calculations and this increased speed decreases the heat flux to the walls.

ACKNOWLEDGEMENT

This work was sponsored by the Air Force Office of Scientific Research under Contract AFOSR 84-0048.

REFERENCES

1. W. R. Briley, H. McDonald and S. J. Shamroth, "A Low Mach Number Euler Formulation and Application to Time-Iterative LBI Schemes", AIAA Journal, Vol. 21, No. 4, Oct. 1983, pp. 1467-1469.

2. E. Turkel, "Fast Solutions to the Steady State Compressible and Incompressible Fluid Dynamic Equations", ICASE Report No. 84-28, NASA Contractor Report 172416, June 1984.

3. C. L. Merkle and D. Choi, "Application of Time-Iterative Schemes to Incompressible Flow", AIAA Journal, Vol. 23, No. 10, Oct. 1985, pp. 1518-1524.

4. C. L. Merkle and Y.-H. Choi, "Computation of Compressible Flows at Very Low Mach Numbers", AIAA Paper 86-0351, AIAA 24th Aerospace Sciences Meeting, January 6-8, 1986, Reno, NV. To appear in AIAA Journal.

5. C. L. Merkle, "Prediction of the Flowfield in Laser Propulsion Devices", AIAA Journal, Vol. 22, No. 8, August 1984, pp. 1101-1107.

6. J. Guerra and B. Gustafsson, "Numerical Method for Incompressible and Compressible Flow Problems with Smooth Solutions", J. Comp. Phys., Vol. 63, 1986, pp. 377-397.

7. Y.-H. Choi and C. L. Merkle, "Computation of Low Mach Number Flows with Buoyancy", Proceedings of the 10th International Conference on Numerical Methods in Fluid Dynamics, Beijing, China, June 23-27, 1986, pp. 169-173.

8. W. R. Briley and H. McDonald, "On the Structure and Use of Linearized Block Implicit Schemes", Journal of Comp. Phys., Vol. 34, 1980, pp. 54-73.

9. R. M. Beam and R. F. Warming, "An Implicit Factored Scheme for the Compressible Navier-Stokes Equations", AIAA Journal, Vol. 16, April 1978, pp. 393-402.

10. C. L. Merkle, G. A. Molvik and E. J.-H. Shaw, "Numerical Solution of Strong Radiation Gasdynamic Interactions in a Hydrogen-Seedant Mixture", J. of Propulsion and Power, Vol. 2, No. 5, September-October 1986, pp. 465-473.

11. J. Douglas and J. E. Gunn, "A General Formulation of Alternating Direction Methods, Part I, Parabolic and Hyperbolic Problems", Numerische Mathematik, Vol. 6, 1964, pp. 428-453.

12. S. P. Vanka, "Block Implicit Calculation of Steady Turbulent Recirculatory Flows", Int. Journal Heat Mass Transfer, Vol. 28, No. 11, 1985, pp. 2093-2103.

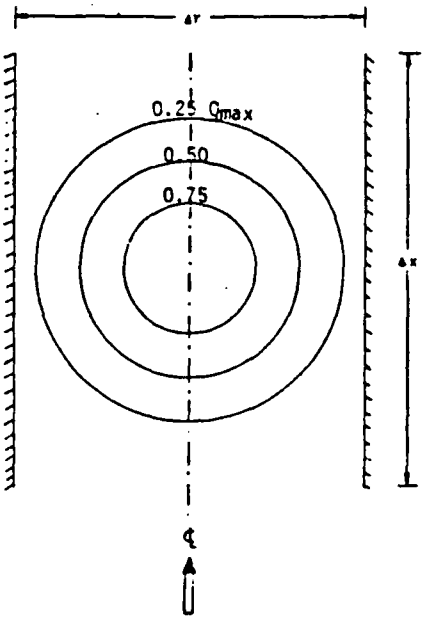

Fig. 1 Schematic of Constant Area Duct Problem Showing Heat Addition Region. Duct Aspect Ratio $\Delta x/\Delta y = 5/4$.

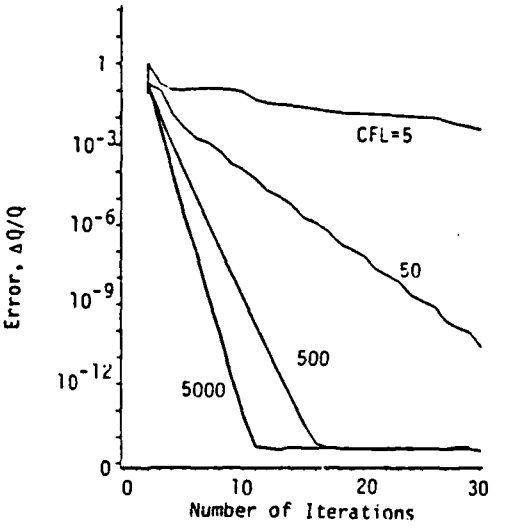

Fig. 2 Convergence of Direct Inversion Algorithm as a Function of CFL.

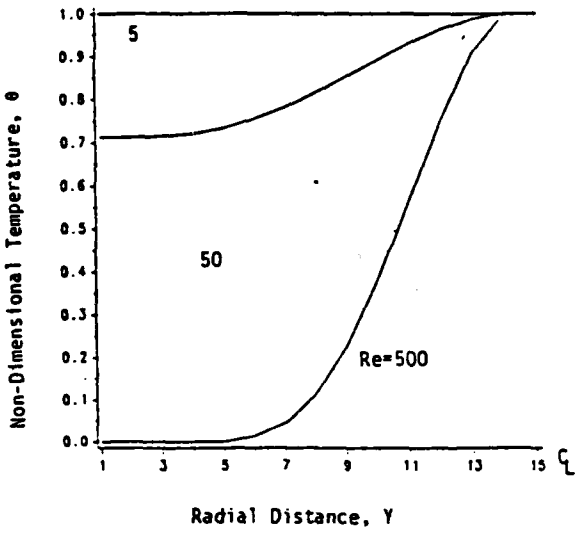

Fig. 3 Nondimensional Temperature Profiles at Exit Plane Without Buoyancy.
$\theta = (T-T_{CL})/(T_{IN}-T_{CL})$

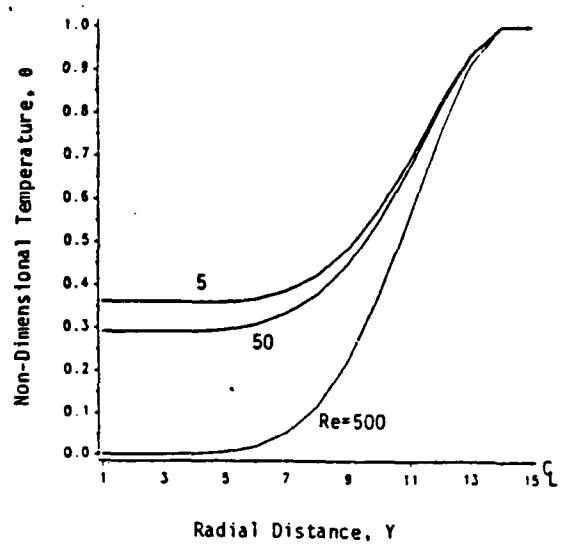

Fig. 5 Nondimensional Temperature Profiles at Exit Plane With Buoyancy.
$\theta = (T-T_{CL})/(T_{IN}-T_{CL})$

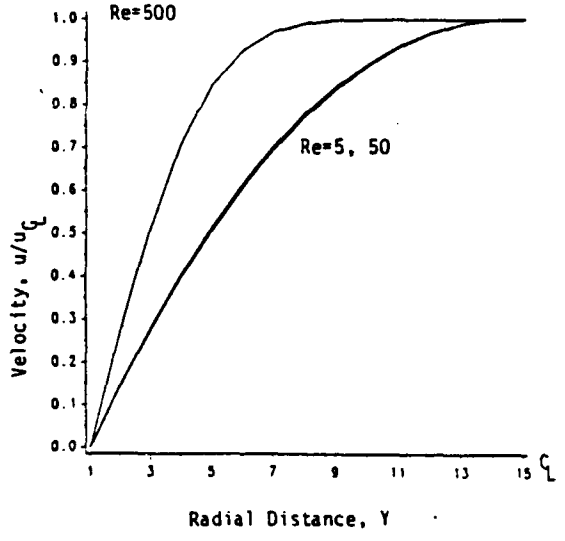

Fig. 4 Nondimensional Velocity Profiles at Exit Plane Without Buoyancy.

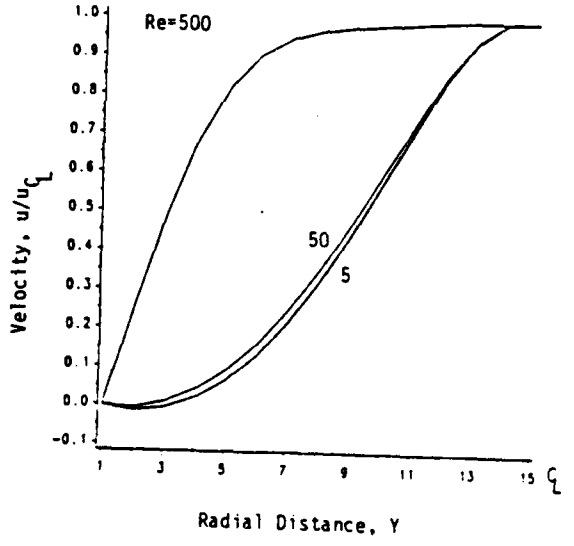

Fig. 6 Velocity Profile at Exit Plane With Buoyancy Effects Included.

END
DATE
FILMED
7-88
DTIC